Subterahertz Superlattice Parametric Oscillator

K. F. Renk,* B. I. Stahl, A. Rogl, and T. Janzen
Institut für Angewandte Physik, Universität Regensburg, 93040 Regensburg, Germany

D. G. Pavel'ev and Yu. I. Koshurinov
Department of Radiophysics, Nizhny Novgorod State University, Nizhny Novgorod, Russia

V. Ustinov and A. Zhukov
A. F. Ioffe Physico-Technical Institute, St. Petersburg, Russia
(Received 10 December 2004; published 13 September 2005)

We report a superlattice parametric oscillator (SPO), with a GaAs/AlAs superlattice as the active element. The SPO was pumped by a microwave field (power 4 mW) and produced third harmonic radiation at subterahertz frequencies (near 300 GHz; 0.1 mW). We attribute the parametric gain to the nonlinearity of the miniband transport.

DOI: 10.1103/PhysRevLett.95.126801 PACS numbers: 73.21.Cd, 05.45.−a, 07.57.Hm, 42.65.Ky

Esaki and Tsu predicted that miniband transport by the conduction electrons in a semiconductor superlattice should lead to a negative differential resistance, making a superlattice suitable for high-frequency applications [1]. Molecular beam epitaxy has been applied for preparation of superlattices with negative differential resistance [2]. A static-voltage biased superlattice in a negative resistance state can be a gain medium for THz radiation as predicted [3] and concluded from a voltage-induced anomalous THz transmissivity of an array of superlattices [4]. An oscillator with a static-voltage biased superlattice as the active element is a candidate for a room-temperature, coherent THz radiation source (see, e.g., Refs. [4,5]); at present, the quantum cascade laser (working at frequencies between 2 and 4 THz), operated at liquid nitrogen temperature, is a first compact coherent THz radiation source [6]. In this Letter, we report the operation of a superlattice parametric oscillator (SPO) for generation of sub-THz radiation. It is pumped by a microwave field and delivers third harmonic radiation at sub-THz frequencies (near 300 GHz). We also discuss the possibility of up-conversion of microwave radiation to the THz frequency range.

The SPO [Fig. 1(a)] contained a SLED (superlattice electronic device) in which the active superlattice was integrated. The SPO was pumped by a microwave field (pump frequency ω_1) and generated third harmonic radiation (frequency ω_3). A resonator (reflector $r1$, partial reflector $r2$) for the third harmonic radiation delivered feedback necessary for parametric oscillation [7,8]. The SPO consisted [Fig. 1(b)] of a double-waveguide structure with a SLED coupled by fin antennas to a third harmonic waveguide resonator and to a pump waveguide; a gold film terminal of the SLED was attached (with a conducting glue) on one antenna, and the other terminal (of the SLED diode) was connected by a metal strip to the other antenna. In the resonator, a fixed backshort and a mismatch between the output port and a horn corresponded to two reflectors ($r1$ and $r2$; distance about 1 cm). Radiation was detected with a frequency mixer connected to a spectrum analyzer or with a power meter. For pumping we used radiation of a frequency synthesizer (frequency range 75 to 110 GHz; maximum power 4 mW). In a modified arrangement [Fig. 1(c)], we produced a parallel beam and

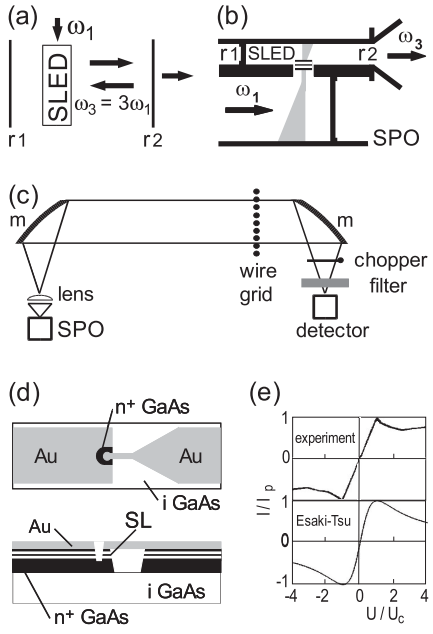

FIG. 1. The superlattice parametric oscillator (SPO). (a) Principle. (b) Experimental arrangement; cross sectional areas 2.54 mm × 1.27 mm (pump waveguide) and 0.8 mm × 0.4 mm (third harmonic waveguide), separation between the waveguides 0.2 mm. (c) SPO coupled to an external resonator with a wire grid partial reflector; m, parabolic mirrors. (d) Superlattice electronic device (SLED); cross sectional and top views. (e) Experimental I-U curve measured with a static-voltage source and Esaki-Tsu curve; I_p (~0.7 mA), peak current (peak current density 200 kV/cm), and U_c (~0.2 V), critical voltage.

focused the radiation on a Golay detector. By placing a partial reflector (a wire grid) into the parallel beam, we obtained a coupled-resonator system with the three reflectors $r1$, $r2$, and grid; by rotating the wire direction relative to the polarization direction of the radiation, it was possible to change the reflectivity of the grid (from almost 0 to almost 1) and thus the feedback by the external resonator.

By molecular beam epitaxy we had grown, on a semi-insulating GaAs substrate, an n^+ GaAs layer (silicon doping 6×10^{18} cm^{-3}; thickness 1.5 μm), a gradual layer (thickness 32 nm), then the superlattice, again a gradual layer and an n^+ InGaAs gradual layer (25 nm) and, finally, an n^+ InGaAs layer (20 nm, doping 10^{19} cm^{-3}); the gradual layers delivered smooth transitions of the doping and the layer thickness. The superlattice (length 112 nm) had 18 periods, each period (length 6.23 nm) with 18 monolayers GaAs and 4 monolayers AlAs and was homogeneously doped with silicon (1×10^{18} cm^{-3}). By use of a photolithographic technique, we prepared SLEDs.

A SLED [Fig. 1(d)] had a quasiplanar design (size 200 μm $\times$ 150 μm; thickness 20 μm). The connection from one film (on the top of a supporting superlattice) to the top of the active superlattice (diameter $\sim$1.5 μm) was provided via a gold bridge (length $\sim$ 10 μm, width $\sim$ 1 μm), which had been obtained by an appropriate underetching process. The other contact film was connected to the bottom of the active superlattice through a low-resistance, large-area superlattice and the n^+ GaAs layer. Different SLEDs showed similar current-voltage (I-U) curves. One is shown in Fig. 1(e) (top). The curve indicates that the SLED and thus the small-area superlattice had an Ohmic resistance near zero voltage and a negative differential resistance above a critical voltage U_c where the peak current (I_p) was reached. We compare the experimental curve with an Esaki-Tsu curve [Fig. 1(e), bottom] described by [1] $I/I_p = 2U/U_c(1 + U^2/U_c^2)^{-1}$. The nonlinearity is a consequence of Bragg reflections of the conduction electrons at the superlattice planes, i.e., of a miniband for the electron motion along the superlattice axis (miniband width $\sim$25 meV and minigap to the next higher band $\sim$70 meV for our superlattice). The critical voltage is determined by the relation $\omega_B \tau = 1$ where τ ($\sim 1.5 \times 10^{-13}$ s) is an average intraminiband electron relaxation time and $\omega_B = \frac{1}{\hbar} eaU_c/L$ is the Bloch frequency, a the period, and L the length of the superlattice ($U_c/L \sim 10$ kV/cm). The experimental curve is in accord with the Esaki-Tsu curve for $U < U_c$ if a resistance ($\sim 10\ \Omega$) in series to the small-area superlattice is taken into account. It deviates for $U > U_c$ because of the occurrence of space charge domains [9], joint with nonuniform electric fields within the superlattice. A high-frequency field acting on a superlattice may lead to either a domain or a single-electron nonequilibrium state. In the domain state, a sub-THz field interacts with transient electron ensembles. A pump field creates and annihilates, during each half cycle, a domain giving rise to a current that is the source of third harmonic radiation. In the single-electron state, the electric field within the active superlattice remains uniform and the electrons interact independently from each other with the field.

A first sign of parametric oscillation was a thresholdlike behavior of the third harmonic signal S_3 (Fig. 2). With increasing pump power (P_1), S_3 varied as P_1^3, showed a stronger increase above P_c and a thresholdlike increase at P_{th} and then saturated [10]. We attribute P_c to a critical pump power, where the amplitude of the pump voltage across the active superlattice exceeded U_c, and associate P_{th} with the threshold for parametric oscillation. Accordingly, the S_3 signal corresponded at low pump power to conventional frequency tripling according to the nonlinear I-U curve, then, at intermediate power levels (between P_c and P_{th}), to frequency tripling without SPO action, most likely domain mediated, and finally (above P_{th}) to SPO action [11]. A change of the reflectivity of the partial reflector ($r2$) resulted in a change of P_{th} (up to 10%) which directly indicated the effect of feedback. The oscillator delivered, at optimum output coupling, a power ($\sim$0.1 mW) which corresponded to an efficiency of 2.5% for conversion of pump to third harmonic radiation.

For a further study of the feedback we used the modified arrangement and determined the third harmonic signal S_3 for different pump, i.e., third harmonic frequencies. The corresponding frequency characteristic obtained without an external resonator is drawn in Fig. 3(a) (left). The characteristic was almost constant at a pump power slightly below P_{th}, then showed (at P_{th}) a narrow peak and extended, for P_1 slightly larger than P_{th}, over a range of about 0.3% of a center frequency; a structure at $P_1/P_{\text{th}} = 1.002$ was due to slightly different pump power levels at different

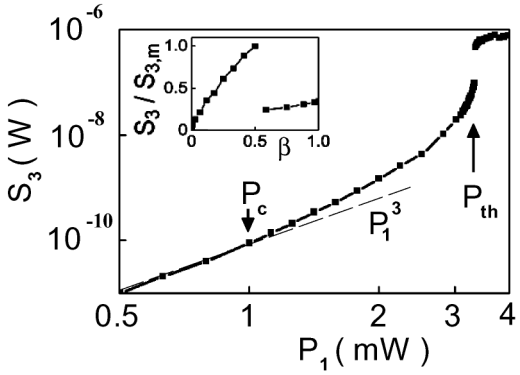

FIG. 2. Third harmonic signal (S_3) for different pump power levels (P_1) at a third harmonic frequency near 291 GHz; P_c, critical pump power corresponding to the onset of negative differential resistance and P_{th}, SPO pump threshold. Inset: S_3 relative to the maximum signal ($S_{3,m}$) at constant pump power ($P_1 \sim P_{\text{th}}$; frequency 290.700 GHz) for different values of the loss $\beta = T = 1 - R$ in the modified arrangement; T, transmissivity, and R, reflectivity of the grid.

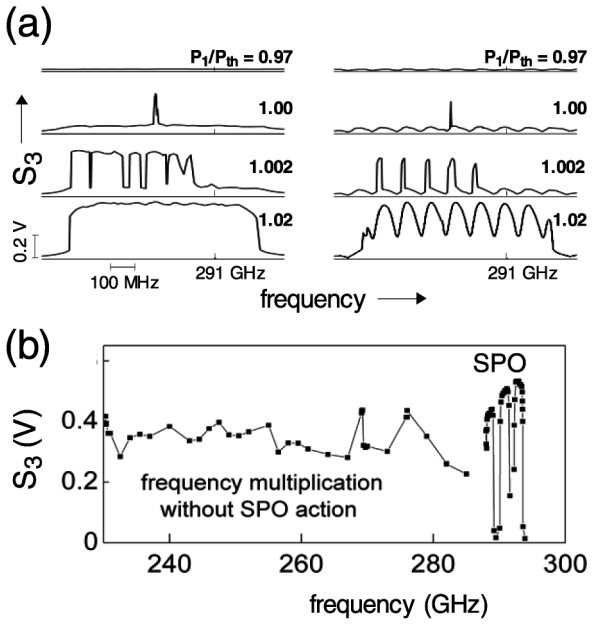

FIG. 3. Frequency characteristics. (a) Characteristics of the SPO without (left) and with (right) external resonator at a grid reflectivity of 0.5. (b) S_3 signal measured over a large frequency range ($P_1 \sim 4$ mW).

frequencies. If we inserted the external reflector, which needed a careful adjustment, the characteristic [Fig. 3(a), right] showed, at threshold, oscillation in a narrow frequency range, and slightly above threshold ($P/P_{\text{th}} = 1.002$) oscillation in narrow frequency ranges (widths $\sim$20 MHz) at a separation ($\sim$100 MHz) of the modes of the external resonator (length $\sim$1.5 m), indicating parametric oscillation; with increasing pump power the oscillation ranges broadened and finally overlapped (right panel, lowest curve). An increase of the reflectivity (from 0.5 to 0.9) of the partial mirror resulted in a decrease of P_{th}, which is a further indication of parametric oscillation; the decrease was, however, small ($\sim$1%) because in our quasioptical arrangement only a portion of the SPO output radiation was coupled to the external resonator. As for lasers and other oscillators, there was an optimum output coupling for the SPO (Fig. 2, inset). With increasing grid transmissivity, i.e., decreasing reflectivity, S_3 increased up to a maximum value and then showed a sharp drop; the S_3 signal at larger transmissivity was due to tripling without SPO action. A power balance, taking into account the reflectivity ($\sim$0.5) at optimum output coupling, showed that a third harmonic photon made in the average about three passages through the active SLED, which corresponded to a gain coefficient for the active superlattice of the order of 10^4 cm^{-1}.

A survey of the frequency characteristic on a large frequency range [Fig. 3(b)] indicated two different regimes that we characterized as non-SPO and SPO ranges. In the non-SPO range, the characteristic was only weakly influenced by an external resonator. The S_3 signal increased, for a fixed frequency, almost continuously with pump power and showed no thresholdlike jump. At large pump power, the S_3 signal saturated and showed only weak frequency dependence.

In the range of SPO action, the S_3 signal was slightly larger and showed the threshold behavior and feedback by an external resonator as discussed; a structure in the frequency characteristic can be attributed to a coupling of the third harmonic field to the pump waveguide. Towards high frequencies, SPO operation was restricted by the pump power we had available. We attribute the S_3 signal in the non-SPO region to domain-mediated frequency multiplication. The SPO action can, in principle, be due to another domain mode or it can be due to a domainless, single-electron nonequilibrium state of the superlattice; i.e., it seems possible that the interplay of the pump field and its third harmonic field leads to a domainless, single-electron nonequilibrium state.

For a discussion of parametric gain we made use, for simplicity, of the Esaki-Tsu current-voltage curve, which allows one to describe a domainless state. In the stationary state of SPO action, a pump and a third harmonic field are synchronously acting on the active superlattice. The fields are joint with voltages across and currents through the superlattice (Fig. 4). A pump voltage ($U_1 = \hat{U}_1 \cos\omega_1 t$) and a third harmonic voltage ($U_3 = \hat{U}_3 \cos\omega_3 t$) add to a total voltage ($U_1 + U_3$). The current (I) calculated by the use of the Esaki-Tsu formula contains a third harmonic Fourier component (I_3) of opposite phase relative to U_3. Accordingly, the resistance for the third harmonic field, $R_3 = \hat{U}_3/\hat{I}_3$, is negative indicating gain, and the power of the third harmonic field, $P_3 = \frac{1}{2}\hat{I}_3\hat{U}_3$, is negative corresponding to the transfer of power from the pump to the third harmonic field. We have varied $\hat{U}_1$ and $\hat{U}_3$ and found that P_3 had a maximum for $\hat{U}_1 \sim 3U_c$ and $\hat{U}_3 \sim U_c$; this

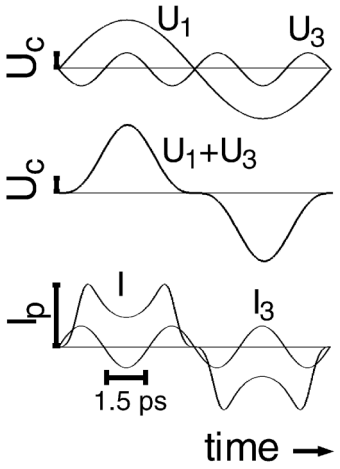

FIG. 4. Voltages and currents involved in the parametric oscillation.

situation is illustrated in Fig. 4. It follows for the optimum efficiency of the conversion of pump to third harmonic power a value of about 10%; the difference to the experiment ($\sim$2.5%) can be attributed to a nonperfect matching of the superlattice to the pump and third harmonic waveguides and to loss of third harmonic radiation to the pump waveguide. The calculation also shows that (for $\hat{U}_1 \sim 3U_c$) P_3 is negative also for small $\hat{U}_3$ and that parametric oscillation can be initiated by a weak third harmonic field which is growing due to the feedback by the resonator until the optimum operation point is reached. A more detailed analysis would have to include domains and appropriate boundary conditions. We note that the parameter characterizing the parametric interaction [12] is the resistance; in the case of domain-mediated gain, the capacity of the superlattice also plays a role.

Our result indicates that the parametric gain was due to the nonlinearity of the miniband transport rather than to the electron transfer from the Γ conduction band of GaAs to side valleys (Gunn effect); this effect would not allow an efficient generation of 300 GHz radiation because of the limitation by the relaxation from the side valleys to the Γ valley (relaxation time few ps).

We guess that SPO action should also be possible in the THz frequency range where $\omega_3\tau > 1$ and where the processes of domain creation and annihilation, limited by electron-phonon interaction [13], are not fast enough to follow the THz field. Then, single-electron interaction with the pump and the third harmonic field can still be the origin of parametric gain, as corresponding studies (unpublished) show. By the use of SPOs in series, up-conversion of microwave radiation to the THz range may be possible. It is a challenge to develop appropriate superlattices and resonators to realize a THz SPO.

The SPO represents a novel type of parametric oscillator, it is based on the nonlinear response of the conduction electrons to an electromagnetic field. The gain cross section per conduction electron ($\sim 10^{-14}$ cm^2 for our superlattice) is by many orders of magnitude larger than in the optic parametric oscillator (OPO) which makes use of bound electrons (see, e.g., Ref. [14]). In the OPO, which produces infrared [15] and far-infrared [16] radiation, each time a high-frequency photon of the pump field is annihilated, two low frequency photons are created, while in the SPO, each time three photons of the pump field are annihilated, a photon of the third harmonic field is created.

In conclusion, we demonstrated the operation of an SPO, with a superlattice as the active medium. We suggest that under appropriate experimental conditions a domain state can be avoided in favor of a single-electron nonequilibrium state. Because of attractive properties, namely, narrow bandwidth, coherence, compactness, room-temperature operation, and the wide tunability, the SPO appears to be a promising optoelectronic device.

The work has been supported by the Deutsche Forschungsgemeinschaft and the Russian Foundation for Basic Research (Project No. 03-02-17088).

*Electronic address: karl.renk@physik.uni-regensburg.de

[1] L. Esaki and R. Tsu, IBM J. Res. Dev. **14**, 61 (1970).
[2] A. Sibille, J. F. Palmier, H. Wang, and F. Mollot, Phys. Rev. Lett. **64**, 52 (1990).
[3] S. A. Ktitorov, G. S. Simin, and V. Ya. Sindalovskii, Fiz. Tverd. Tela **13**, 2230 (1971) [Sov. Phys. Solid State **13**, 1872 (1972)].
[4] P. G. Savvidis, B. Kolasa, G. Lee, and S. J. Allen, Phys. Rev. Lett. **92**, 196802 (2004).
[5] H. Kroemer, cond-mat/0007482 (unpublished); E. Schomburg, N. V. Demarina, and K. F. Renk, Phys. Rev. B **67**, 155302 (2003).
[6] R. Köhler *et al.*, Nature (London) **417**, 156 (2002); L. Mahler *et al.*, Appl. Phys. Lett. **84**, 5446 (2004); J. Alton *et al.*, Appl. Phys. Lett. **86**, 071109 (2005).
[7] An idea of a microwave pumped superlattice oscillator has been published earlier: F. Klappenberger and K. F. Renk, Int. J. Infrared Millim. Waves **25**, 429 (2004).
[8] K. Alekseev informed us about earlier work on parametric interaction; V. V. Pavlovich, Fiz. Tverd. Tela **19**, 97 (1977) [Sov. Phys. Solid State **19**, 54 (1977)], predicted the amplification of a weak high-frequency field in a superlattice submitted to a strong pump field; Yu. A. Romanov, Izv. Vyssh. Uchebn. Zaved., Radiofiz. **23**, 617 (1980) [Radiophys. Quantum Electron. **23**, 421 (1980)], considered parametric generation of uneven harmonics in a superlattice under the condition of a strong nonlinearity.
[9] H. Kroemer, Proc. IEEE **58**, 1844 (1970); M. Büttiker and H. Thomas, Phys. Rev. Lett. **38**, 78 (1977); A. A. Ignatov, V. I. Piskarev, and V. I. Shashkin, Sov. Phys. Semicond. **19**, 1345 (1985); K. Hofbeck *et al.*, Phys. Lett. A **218**, 349 (1996); for a discussion of domains see also Ref. [4].
[10] The investigation of a (very weak) leakage signal through the SPO indicated that the pump power P_1 increased smoothly near P_{th} and that therefore the jump in S_3 was due to the parametric oscillation and not to a jumplike increase of the matching of the pump field to the superlattice.
[11] F. Klappenberger, K. F. Renk, P. Renk, B. Rieder, Yu. I. Koschurinov, D. G. Pavel'ev, V. Ustinov, A. Zhukov, N. Maleev, and A. Vasilyev, Appl. Phys. Lett. **84**, 3924 (2004), attributed a threshold behavior of a frequency tripler to the onset of domain formation rather than to an oscillation.
[12] D. W. H. Louisell, *Radiation and Noise in Quantum Electronics* (Krieger Publishing Company, New York, 1977).
[13] F. Klappenberger *et al.*, Eur. Phys. J. B **39**, 483 (2004).
[14] R. W. Boyd, *Nonlinear Optics* (Academic Press, New York, 2003); G. P. Agrawal, *Nonlinear Fiber Optics* (Academic Press, New York, 1989).
[15] I. M. Bayanov *et al.*, Opt. Commun. **113**, 99 (1994).
[16] K. Kawase *et al.*, Appl. Phys. Lett. **68**, 2483 (1996).